

Dynamic Polymer Networks

How to cite: *Angew. Chem. Int. Ed.* **2021**, *60*, 13725–13736

International Edition: doi.org/10.1002/anie.202013254

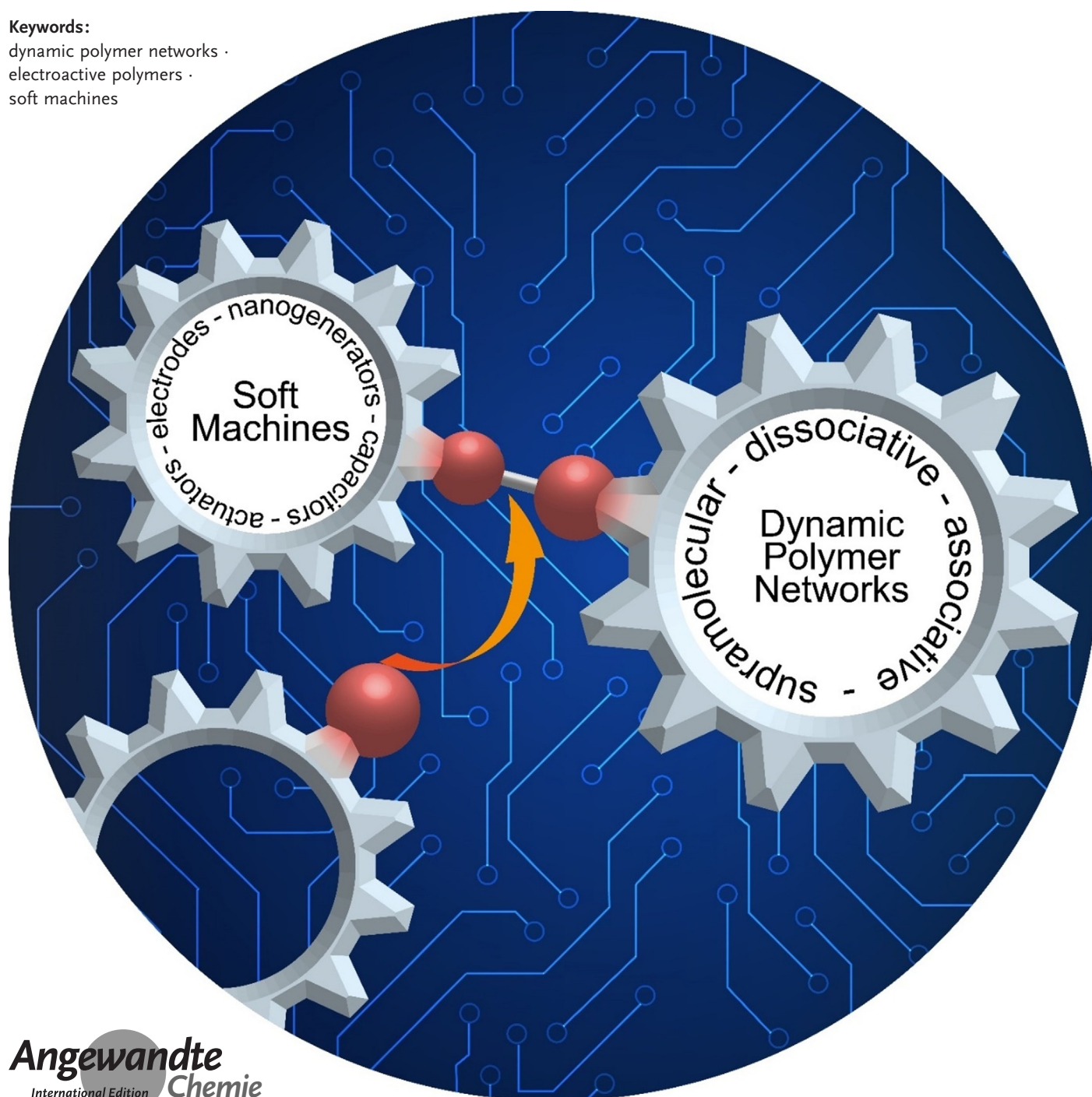
German Edition: doi.org/10.1002/ange.202013254

Dynamic Polymer Networks: A New Avenue towards Sustainable and Advanced Soft Machines

Alan M Wemyss, Christopher Ellingford, Yoshihiro Morishita, Chris Bowen,* and Chaoying Wan*

Keywords:

dynamic polymer networks ·
electroactive polymers ·
soft machines



While the fascinating field of soft machines has grown rapidly over the last two decades, the materials they are constructed from have remained largely unchanged during this time. Parallel activities have led to significant advances in the field of dynamic polymer networks, leading to the design of three-dimensionally cross-linked polymeric materials that are able to adapt and transform through stimuli-induced bond exchange. Recent work has begun to merge these two fields of research by incorporating the stimuli-responsive properties of dynamic polymer networks into soft machine components. These include dielectric elastomers, stretchable electrodes, nanogenerators, and energy storage devices. In this Minireview, we outline recent progress made in this emerging research area and discuss future directions for the field.

1. Introduction

For centuries, machines and devices have been developed to assist in the undertaking of work in applications such as manufacturing, construction, and healthcare. During this time, significant advances in materials science, engineering, and computation have led to the creation of complex assemblies of rigid materials that are capable of carrying out the most intricate of tasks. However, there are specific application areas where the use of these advanced machines has been limited. This is, in part, because of the high density, high hardness, and low compliance of the materials that they are made from, which confine them to a single specific task. It can also make them energy inefficient during operation, and make them dangerous to use alongside, or when interacting with, humans. In response to these limitations, there has been intensive research effort in recent years towards the development of soft machines^[1] that can consist of soft components, such as sensors,^[2] actuators,^[3] and energy generators.^[4]

From a materials perspective, since the 1990s, silicone, acrylic (3M™ VHB™), and polyurethane have been the dielectric elastomers most commonly used in soft machine applications due to their large mechanical strain to failure (300–900%), high energy density (10–150 kJ m⁻³), and rapid response (10⁻³ s).^[5] However, these materials possess intrinsic limitations to their performance, such as low relative permittivity ($\epsilon_r = 2-10$), high viscous losses, and poor tear resistance. In addition, stress-relaxation and creep strongly influence the behaviour of elastomers during stress cycling, as the energy from an applied mechanical strain is dissipated through a variety of mechanisms, such as polymer chain movement and chain disentanglement. This gives rise to hysteresis effects that reduce the energy required to strain these elastomers, often resulting in mechanical and electromechanical instabilities that make them more susceptible to failure over time.^[6] The lifetime of these materials can be enhanced by operating at low strains to prevent damage,^[7] or by introducing cross-links that simultaneously inhibit creep, whilst retaining high strain properties. Device efficiency is benefitted by the latter strategy, however, the permanent nature of conventional

covalent cross-links is detrimental to the sustainability of these materials, since they limit the potential for recycling.^[8]

To overcome this challenge, the emerging chemistry of dynamic polymer networks (DPNs) is shedding light on a new generation of smart and reprocessable materials. These systems consist of dynamic interactions that allow for rearrangements of their network topology and adaptation of their properties in response to an environmental stimulus.^[9] The cross-linking of DPNs can be covalent or non-covalent, and the materials they form may be classified as either dissociative, associative, or supramolecular networks, depending on the exchange chemistry

of their dynamic bonds, as summarised in Figure 1. Dissociative networks, illustrated in Figure 1 a, possess an equilibrium between the association and dissociation of their cross-links. After the formation of the network, the equilibrium can be shifted towards dissociation through the application of an external stimulus, such as heat or light, which decreases the cross-link density and eventually results in the formation of free polymer chains. In contrast, associative networks, sometimes termed vitrimers,^[10] respond to these stimuli by undergoing exchange reactions, such as those given in Figure 1 b, which facilitates bond exchange whilst also maintaining a constant number of cross-links in the network.^[11] Supramolecular networks have the same exchange mechanism as dissociative networks but are formed when molecules are linked through physical associations; for this Minireview we will specifically refer to their formation between macromolecules, as shown in Figure 1 c.

In a similar way to conventional covalent cross-links, dynamic covalent bonds can reduce creep in elastomers,^[8b] whilst also allowing efficient reprocessing of the material and

[*] Dr. A. M. Wemyss, C. Ellingford, Dr. C. Wan
International Institute for Nanocomposites Manufacturing (IINM)
WMG, University of Warwick, Coventry, CV4 7AL (UK)
E-mail: chaoying.wan@warwick.ac.uk

Prof. C. Bowen
Department of Mechanical Engineering
University of Bath, Bath, BA2 7AY (UK)
E-mail: msscrb@bath.ac.uk

Dr. Y. Morishita
Core Technology Research Department
Advanced Materials Division, Bridgestone Corporation (Japan)

 The ORCID identification number(s) for the author(s) of this article can be found under:

<https://doi.org/10.1002/anie.202013254>.

 © 2021 The Authors. Angewandte Chemie International Edition published by Wiley-VCH GmbH. This is an open access article under the terms of the Creative Commons Attribution Non-Commercial License, which permits use, distribution and reproduction in any medium, provided the original work is properly cited and is not used for commercial purposes.

imparting self-healing functionality.^[12] Supramolecular interactions can also contribute to the formation of a creep resistant elastomer, however, since their bond strength is typically lower than dynamic covalent bonds these linkages are less effective in reducing creep.^[13] The creation of specific combinations of dynamic covalent bonds and supramolecular interactions has a high potential to generate autonomously self-healing, reprocessable, and low creep elastomers,^[14] which are electromechanically stable, have a high extensibility, and can be subjected to large applied electric fields with a reduced likelihood of premature failure.

There are several excellent reviews on the synthesis and characterisation of DPNs,^[15] ranging from the polymerisation of functional monomers to the functionalisation of commercial elastomers. Emerging work on the application of DPNs in fields such as polymeric actuators, engineering rubbers, and tissue engineering has also been recently reviewed.^[16] However, ongoing research is demonstrating that the adaptive and reprocessable features of DPNs offer new opportunities for next generation electroactive polymers for smart soft ma-

chines. It is therefore timely to analyse the potential for exploiting DPNs in stretchable electronics and soft machine applications, including dielectric elastomers, flexible and stretchable electrodes, nanogenerators, and soft components for energy storage. For each application we will critically evaluate the design strategies of the DPNs, and how the mechanisms of exchange can influence the electromechanical, thermomechanical, and electrochemical performance of the materials and devices.

2. Dielectric Elastomers

The key mechanical and electrical properties of interest for dielectric materials in electrical storage, actuation, and harvesting applications are their Young's modulus (Y), electrical breakdown strength (E_b), relative permittivity (ϵ_r), and dielectric loss, often defined by $\tan\delta$. The actuation properties of dielectric elastomers can be evaluated by considering a relevant performance figure of merit,



Alan M. Wemys is a Research Fellow at the International Institute for Nanocomposites Manufacturing (IINM), WMG, University of Warwick. He received his BSc (2009) from the University of Glasgow and PhD (2016) from the University of Warwick, UK. His current research focusses on the design and synthesis of new dynamic polymer networks for a range of applications.



Christopher Rhys Bowen has a BSc degree in Materials Science from the University of Bath (1986–1990) and a DPhil in Ceramics from the University of Oxford (1990–1993). Post-doctoral work has been undertaken at Technische Universität Harburg-Hamburg and University of Leeds (1994–1996). He was Senior Scientist at the Defence Evaluation and Research Agency from 1996–1998. He is now a Professor of Materials at the University of Bath. Research areas include energy harvesting, piezoelectric materials, dielectrics, and functional ceramics.



Christopher Ellingford received his 1st class MChem in Chemistry from the University of Warwick in 2016. He completed his Ph.D. under Dr Chaoying Wan in the International Institute for Nanocomposites Manufacturing (IINM), WMG, at the University of Warwick in 2020, where he is now a Postdoctoral Research Fellow. His research interests include biodegradable polymers and nanocomposites for flexible packaging applications and self-healing dielectric elastomers for energy harvesting and actuation devices.



Chaoying Wan received her PhD degree in Materials Science from Shanghai Jiao Tong University. She was awarded a Marie Curie Individual Fellowship and worked at Trinity College Dublin, Ireland. She joined the University of Warwick in 2012, where she is currently a Reader in multifunctional nanocomposites. She specializes in polymer synthesis, polymer characterization, the reactive processing of multiphase/multicomponent nanocomposites, smart dielectric elastomers, biodegradable polymers, and sustainable rubbers for energy applications.



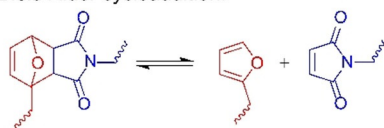
Yoshihiro Morishita is a researcher/engineer in the Core Technology Research Department, Advanced Materials Division at Bridgestone Corporation. He received his bachelor and master degrees in applied physics from the University of Tokyo and joined Bridgestone in 2009. He investigated rubber compounds in Bridgestone, and then received his PhD from the Kyoto Institute of Technology on fracture dynamics of elastomers (2017). His current research interests include the mechanical properties, durability, and advanced functions (e.g. self-healing) of polymer composites.

a) Dissociative networks

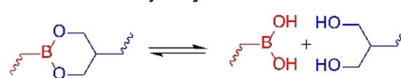
General Mechanism:



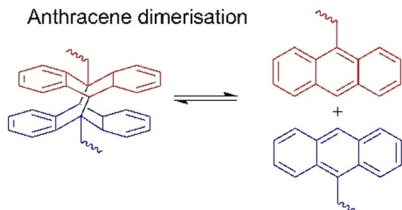
Diels-Alder cycloaddition:



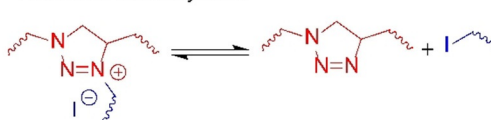
Boronic ester hydrolysis:



Anthracene dimerisation



Triazolium transalkylation



b) Associative networks

General Mechanism:



Vinylogous urethane transamination:



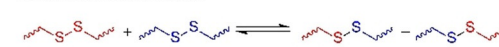
Transesterification:



Imine transamination:

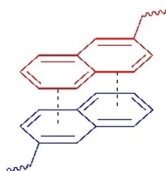


Disulfide metathesis:

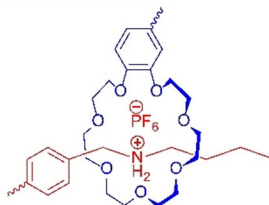


c) Supramolecular networks

π - π interactions:



Host-guest interactions:



Metal ligand coordination:



Hydrogen bonding:

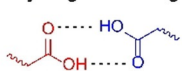


Figure 1. Illustration of important bonds found in a) dissociative networks, b) associative networks, and c) supramolecular networks.

$F_{ac} = \frac{\epsilon_0 \epsilon_r E_b^2}{Y}$, where a low stiffness, Y , facilitates material deformation and actuation under the applied field. For applications related to electrical storage and energy harvesting, by exploiting the change in capacitance of the materials with strain, the relevant figure of merit is expressed as $F_{ch} = \epsilon_0 \epsilon_r E_b^2$. In these applications, the high permittivity provides a large polarisation and a high breakdown strength facilitates the application of large electric fields.

For both actuation and energy harvesting, the figures of merit F_{ac} and F_{ch} indicate that high electrical stresses are desirable to maximise energy generation from the device, and thus a high E_b in the material is required to prevent failure.

Typically, polymers have a higher dielectric loss and breakdown strength ($E_b > 500 \text{ MV m}^{-1}$) than dielectric ceramic materials, however, they have an intrinsically low permittivity ($\epsilon_r = 2\text{--}10$). To reduce the electric field at which these systems operate, increasing their relative permittivity is necessary, whilst retaining a high strength, large elastic strain, and high electrical breakdown strength.

The incorporation of electroactive fillers into these materials can enhance the relative permittivity of elastomer composites,^[17] although this extrinsic approach is often at the expense of reducing E_b and shortening the service life of the material, since fillers lead to an increased Y and act to concentrate both the electric field and the mechanical stress

due differences between the permittivity and stiffness of the individual materials. These issues are compounded by inhomogeneous dispersion of the filler within the polymer matrix. Chemical treatment or surface functionalisation of electroactive fillers can help the dispersion and interfacial interactions with polymer matrices, resulting in improved electro-mechanical properties and processability.^[18] For example, introducing low molecular weight polyethylene glycol (e.g. PEG 600) and graphene oxide (GO) to a polyurethane elastomer (TPU) led to the in situ partial reduction of GO (rGO), which was well dispersed in the TPU through hydrogen bonding interactions with PEG.^[19] This “rearrangement” of the hydrogen bonding interactions in the composite simultaneously led to an enhanced relative permittivity for the composites, from $\epsilon_r \approx 7$ for pristine TPU to $\epsilon_r \approx 71$ for the TPU/PEG/rGO (100/30/1.5 phr), as well as a lower Young’s modulus.^[19]

A different approach to increasing permittivity is the direct grafting of organic dipoles to the polymer chains. This intrinsic approach to enhancing the ϵ_r of materials can maintain their mechanical flexibility and high breakdown strength.^[5] For example, polar groups capable of hydrogen bonding or electrostatic interactions increase the relative

permittivity of the material, whilst also introducing self-healing and re-processability through the formation of a supramolecular network.^[5] In this strategy, the optimal degree of functionalisation needs to be considered to balance mechanical and electrical performance.^[20]

Figure 2 summarises how the introduction of different functional groups to polymer backbones affects their elastic modulus, breakdown strength, and relative permittivity for electroactive behaviour. The introduction of polar groups, such as amines and organic acids, to silicone polymers increased the relative permittivity whilst decreasing the elastic modulus and dielectric breakdown strength. This can be observed clearly for TG-silicone where the grafting of thioglycolic acid (TG) increased the relative permittivity from $\epsilon_r = 3.6$ to 6, but decreased the elastic modulus and breakdown strength from $Y = 0.21$ MPa to 0.05 MPa and $E_b = 38$ V μm^{-1} to 20 V μm^{-1} , respectively. All of the modified silicone elastomers had a lower breakdown strength and low elastic modulus compared to pristine silicone, and the lower elastic modulus significantly contributes to the high actuation performance of the modified silicone elastomers.

Compared with silicone, the elastic modulus of poly(styrene-butadiene-styrene) (SBS)-based elastomers is an order of

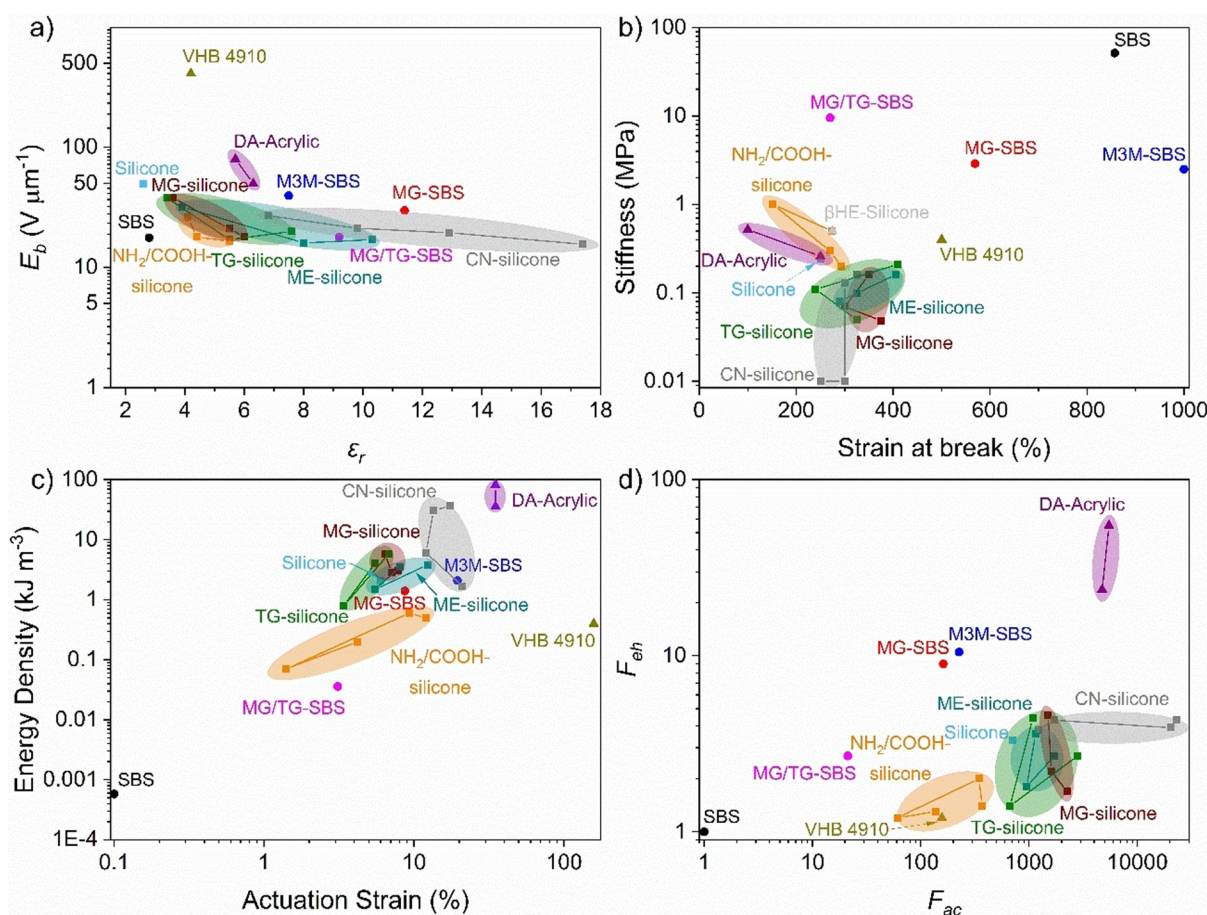


Figure 2. Graphs showing relationships between a) dielectric breakdown strength (E_b) and relative permittivity (ϵ_r); b) stiffness and strain at break; c) energy density and actuation strain; and d) figure of merit for energy harvesting and figure of merit for actuation for SBS-based elastomers (circles), silicone-based elastomers (squares), and acrylic-based elastomers (triangles). The data for each of the materials were taken from: NH_2/COOH -silicone,^[21] SBS,^[20b] silicone, M3M-SBS,^[20c] MG-SBS,^[20b] MG/TG-SBS,^[20a] DA-acrylic,^[22] CN-silicone,^[20e] VHB-4910,^[23] ME-silicone,^[20d] MG-silicone,^[20d] TG-silicone.^[20d]

magnitude greater. The coupling of polar groups to the backbone of SBS has led to a decrease in its elastic modulus, to a minimum of $Y = 2.5$ MPa for SBS modified with methyl-3-mercaptopropionate (M3M-SBS). However, the modified SBS elastomers also exhibited an increased breakdown strength compared to the neat polymer, enhancing both their actuation and energy harvesting performance. Comparing M3M-SBS with SBS modified with methyl thioglycolate (MG-SBS), the lower elastic modulus of M3M-SBS allowed it to actuate up to 9.3% under an electric field of $39.6 \text{ V } \mu\text{m}^{-1}$ and harvest up to 11.5 mJ g^{-1} from a simple energy harvesting device, whereas MG-SBS actuated only 4.2% under an electric field of $29.8 \text{ V } \mu\text{m}^{-1}$ and harvested 2.3 mJ g^{-1} . These studies investigated both the mechanical self-healing and the electrical self-healing of the styrenic elastomers. Mechanically, these elastomers were able to partially self-heal at room temperature, with a strain at break recovery of up to 26% after three days. Self-healing was induced by a weak electrostatic interaction between the $\delta + \text{CH}$ and $\delta -$ aromatic centres of the grafted esters and styrene rings, respectively. In addition, a recovery in the breakdown strength and actuation performance of up to 86% was observed for these materials.^[20b,c] A hydrogen bonding network that enhanced self-healing at elevated temperatures was introduced into MG-SBS via the simultaneous grafting of thioglycolic acid (TG). At 80°C , the elastomer demonstrated a mechanical self-healing efficiency of up to 79% after three hours, highlighting its potential for use in elevated temperature environments. However, its mechanical stiffness was too high ($Y = 9.6$ MPa) for an efficient actuation performance at room temperature.^[20a]

The acrylic elastomer VHB exhibits a relative permittivity of $\epsilon_r = 4.6$, a high breakdown strength and a low elastic modulus. From Figure 2, the incorporation of a dissociative covalent network into this type of dielectric elastomers provided control over important properties that effect a material's actuation potential, such as its modulus, in addition to increasing the relative permittivity to $\epsilon_r = 6.3$.^[22] In this example, an acrylic dielectric elastomer was synthesised from *n*-butyl acrylate (*n*-BA), di(ethylene glycol) ethyl ether acrylate (EOEA), and 2.5–10 wt% of an acrylic monomer containing a furan–maleimide adduct (FM-A).^[22] Following the addition of a tetrafunctional furan cross-linker, FM-A was able to participate in reversible Diels–Alder cycloadditions that allowed the elastomers to reversibly switch from a hard state to a soft state by varying the temperature. Using this strategy, the elastic moduli of these materials could be varied between $0.2 \leftrightarrow 0.01$ MPa, when 2.5 wt% of FM-A was used, or $2.24 \leftrightarrow 1.32$ MPa using 10 wt% of FM-A. Here, the dissociative network is the key factor in controlling the cross-link density of the material and gaining control over these property changes. In particular, the presence of dissociative networks, where there is a different energy barrier to both the association and dissociation reactions, allows the material to be fixed at a high or low cross-link density by exposure to a unique stimulus. Photo-responsive systems are particularly suited for this purpose, as the forward and reverse reactions can be induced by different wavelengths of light with a high degree of control. For example, polymers conjugated with

anthracene undergo a [4+4] cycloaddition upon irradiation with light at wavelengths > 300 nm to form dimeric anthracene, but exposure to light with a higher energy (< 300 nm) induces a retro-cycloaddition, releasing the free polymer chains.^[24] The coupling of this type of photosystem with the supramolecular bonds discussed above can be a highly effective strategy to balance the electrical and mechanical performance of dielectric elastomers in both actuation and energy harvesting applications.

3. Flexible and Stretchable Electrodes

In addition to dielectric elastomers, compliant conductive electrodes are a key component for actuation and energy harvesting in soft machines applications. Traditional electrodes based on conductive materials are rigid and susceptible to cracking during stretching and early compliant electrodes, such as conductive carbon grease, are easily damaged through contact. Interesting approaches to increasing the flexibility and durability of electrodes through their structural design have emerged in recent years, ranging from simple spring structures to elaborate networks based on kirigami or the art of paper cutting.^[25] However, recent research has focussed on new materials to increase not only the flexibility of electrodes, but also their stretchability, where the introduction of DPNs enables recovery of electrical properties after mechanical damage.^[26]

Polydimethylsiloxane (PDMS) is a good base material for elastomeric electrodes, again due to its relatively low Young's modulus ($Y < 1$ MPa), which ideally should remain low after the addition of conductive fillers.^[5] However, repeated stretching and abrasion leads to mechanical damage that reduces electrode performance, and research is ongoing to create self-healing elastomeric electrodes that are able to recover both mechanical properties and conductivity after damage. Deng et al. showed that by combining a polyborosiloxane (PBS) supramolecular network with a PDMS cured by hydrosilylation and conductive silver nanowires and flakes, the mechanical, electrical, and self-healing properties of the material could be tuned.^[27] The mechanical strength increased as the proportion of cured PDMS increased, and damaged materials recovered 88% of their mechanical properties with 15% PDMS after 12 hours at 60°C . At the self-healing conditions, a viscous flow within these materials transferred the silver nanowires and polymer matrix to the failure site, which allowed for 100% recovery of electrical properties within 20 minutes.^[27] The incomplete recovery of mechanical properties in this case is likely due to the presence of "static" covalent bonds in the network from the cured PDMS. Further improvements in recovery could be examined by using a higher proportion of the PBS supramolecular network, at the cost of some mechanical strength, or by introducing dynamic covalent bonds, which could facilitate higher levels of recovery with minimal change to self-healing conditions.^[15f,28]

An area where soft machines have their highest potential is during operation in conditions where rigid machines would lack efficiency and durability; for example, in undersea

applications where the buoyancy of polymers would reduce their energy cost for operation.^[1] However, these extreme conditions can pose particular challenges for incorporating dynamic bonds into these systems. Guo et al. have sought to address this issue by developing a conductive elastomeric electrode that was able to recover both its mechanical and electrical properties after damage whilst being exposed to a range of harsh conditions.^[29] The elastomer was synthesised from the step growth polymerisation of hydroxy-terminated PDMS, isophorone diisocyanate (IP), 4-aminophenyl disulfide (SS), and bis(hydroxymethyl)-2,2'-bipyridine (BNB), creating a PDMS-SS-IP-BNB network that spontaneously cross-linked through aromatic disulfides and multiple hydrogen bond interactions with different strengths, as illustrated in Figure 3a. To demonstrate the synergistic effect of combining these multiple dynamic bonds, two separate networks were prepared that left out either the strong hydrogen bonds (PDMS-SS-IP) or the disulfide bonds (PDMS-IP-BNB). It can be observed in Figure 3b that cut pieces of the PDMS-SS-IP-BNB elastomer had excellent self-healing efficiencies across a range of environments, recovering 93% of their mechanical properties while underwater and 89% in a 30% NaCl solution. However, in the absence of strong hydrogen bonds, the recovery of the materials was significantly lower in salt water, as well as in acidic environments (pH 0) and at low temperatures (-40°C). In the absence of disulfides, there was

a dramatic reduction in self-healing efficiency for nearly all of the environments tested. After encapsulating a eutectic gallium–indium liquid metal in the PDMS-SS-IP-BNB elastomer it became electrically conductive, even under a 400% strain and after being cut and self-healed, as shown in Figure 3c. This raises the exciting prospect of developing dielectric elastomer electrodes that can be used in a range of extreme electronic environments.^[29]

Hydrogels represent an alternative material that is suitable for a variety of electroactive applications, in particular for wearable or implantable products due to their mechanical similarity with biological tissue.^[30] However, they can be prone to mechanical damage and therefore significant effort has focussed on self-healing hydrogels to recover their properties after failure and improve reliability.^[31] A common strategy to introduce self-healing properties into hydrogels is to introduce boronic ester cross-links.^[32] Boronic esters are able to undergo associative transesterification reactions, or more commonly in hydrogels, dissociatively exchange via hydrolysis to a diol and boronic acid, as shown in Figure 1a.^[33] Wei et al. dispersed conductive polypyrrole (PPy) nanotubes in a polyvinyl alcohol (PVA)–borax matrix to form a highly stretchable ($>1000\%$) conductive hydrogel.^[34] The network of hydrogen bonds within the matrix facilitated the uniform dispersion of PPy, which benefitted the specific capacitance of the electrode, measured at 233.2 F g^{-1} , and its mechanical properties. After damage, the hydrogels were able to self-heal within 15 seconds through hydrogen bonding and the formation of new boronic esters, which allowed for the full restoration of their electrical conductivity. However, their low mechanical strength has thus far limited the potential applications of conductive hydrogel DPNs. The strength of hydrogels can be dramatically enhanced by combining permanent covalent bonds with dynamic bonds, such as terpyridine– Zn^{2+} metal–ligand coordination complexes, which are illustrated in Figure 1c.^[35] Such a strategy could retain the benefits of dynamic bonds to electrical performance, such as in homogeneously dispersing conductive fillers, but would reduce the self-healing efficiency of the materials.

Associative DPNs have also been incorporated into electrode materials.^[36] These materials possess a unique thermal transition temperature, the topology freezing transition temperature (T_v), in addition to the glass transition temperature (T_g). The T_v denotes the temperature at which the rate of associative bond exchange exceeds the rate of material deformation, and the fully cross-linked network begins to flow like a viscoelastic liquid. Electrode materials fabricated from associative DPNs are therefore unique, in that their T_v can be exploited to provide additional benefits such as high temperature self-healing and shape memory performance. For example, the shape of exchangeable liquid crystal elastomers (xLCE) containing β -hydroxy esters can be programmed by heating the material above their T_v under a uniaxial strain.^[37] Here, the mesogenic regions of the xLCE align through transesterification reactions, and the shape of the materials may then be altered by heating and cooling around their isotropic transition temperature (T_i). Wang et al. aligned carbon nanotube sheets (ACNTS) on the surface of

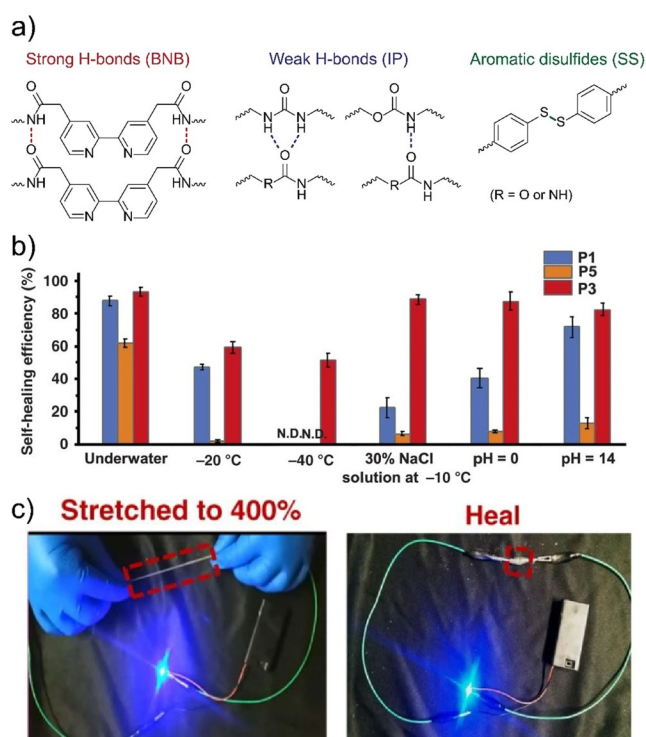


Figure 3. a) Structure of the dynamic bonds present in a self-healing PDMS-SS-IP-BNB elastomer; b) healing efficiencies of PDMS-SS-IP-BNB (labelled P3) under extreme environmental conditions compared with PDMS-SS-IP (labelled P1) and PDMS-IP-BNB (labelled P5); c) demonstration of conductivity of a device based on PDMS-SS-IP-BNB under strain and after self-healing. Adapted with permission from Ref. [29].

an epoxy-acid xLCE to produce electrically conductive films.^[38] Interestingly, these films could self-heal after damage in 3 min by applying a potential difference of 13 V, and recover almost all of their mechanical and electrical properties. Here, self-healing was induced by the electro-thermal properties of the materials, where the heat generated by the applied voltage increases the rate of transesterification. In addition, these electro-thermal processes were shown to control the shape change processes of the LCE, with no increase in the electrical resistance of the material.

4. Nanogenerators

Flexible triboelectric nanogenerators (TENGs) generate electrical energy from periodic contact electrification between two dissimilar material surfaces, at least one of which is coupled to a conductive electrode, as illustrated in Figure 4a. Since their initial design by Wang et al.,^[39] the power density and output voltage of TENG devices has increased by over two orders of magnitude,^[40] making them promising candidates for self-powered soft machines. Recently, there has been a growing effort to incorporate DPNs into TENG devices, thereby providing a number of advantages. Dai et al. fabricated a TENG electrification layer from PDMS cross-linked through dynamic imine bonds and hydrogen bonding between urea and ureidopyrimidone (UPy) groups present in the network (IU-PDMS).^[41] The electrode layer was a nanocomposite prepared from polypropylene glycol, cross-linked with the same dynamic bonds, and filled with UPy-functionalised carbon nanotubes (MWCNTs-UPy/IU-PAM). At room temperature, both layers were able to self-heal after damage, with a full recovery of their mechanical properties within 24 hours. The TENG device was fabricated by sandwiching the MWCNTs-UPy/IU-PAM electrode layer between two IU-PDMS layers, one insulating layer and another that underwent electrification when in contact with human skin, generating a maximum power density of 300 mW m^{-2} , a maximum open circuit voltage (V_{oc}) of 95 V, and a peak short circuit current (I_{sc}) of $9.5 \mu\text{A}$.^[41] Here, the use of DPNs provided three key benefits: (i) any loss of electrical output as a result of frictional damage to the electrification layer could be restored through self-healing; (ii) the shape of the device could be tailored by cutting and remoulding, without loss of properties; and (iii) the compatible dynamic bonds in the multilayer structures facilitated seamless bonding between device layers.

The high interfacial adhesion in multi-layered devices that are subject to movement and friction, such as TENGs, is critical for their long term performance. Chen et al. developed a high-toughness PDMS electrification layer that was cross-linked through hydrogen bonding between urea and urethane groups (A_x-H_{10-x}).^[42] The A_x-H_{10-x} network was able to bond strongly with the UPy groups in the electrode layer, allowing for operation at 16000 cycles of repeated contact-separation with no loss in V_{oc} output (approx. 12 V). Furthermore, when normalised for contact areas, this device maintained its V_{oc} up to an 800% strain, including after being cut and healed, as shown in Figure 4b. Similarly, triboelectric

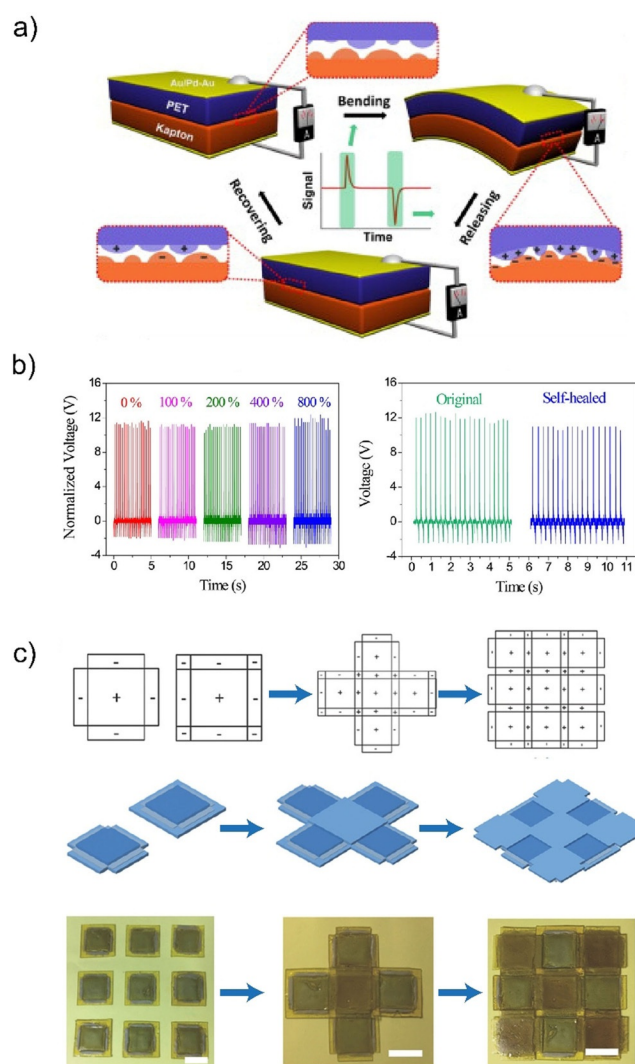


Figure 4. a) Schematic of the working mechanism of a TENG device, adapted with permission from Ref. [39]; b) V_{oc} output of a supramolecular TENG under strain (left) and before and after self-healing (right), adapted with permission from Ref. [42]; c) demonstration of TENG devices based on an associative DPN being built up from identical TENG “bricks”, adapted with permission from Ref. [43].

materials fabricated from metal–ligand pincer complexes, combined with sodium–alginate-based hydrogel electrodes, have been shown to maintain a high electric output ($V_{oc} = 95\text{--}145 \text{ V}$) under large strains and can be cut and self-healed five times, without loss of performance.^[44]

As demonstrated in the examples above, the ability of triboelectric DPNs to self-heal and recover their mechanical and electrical properties is a particular advantage, as these devices can be readily damaged due to the frequent surface contact and friction they are subjected to. However, self-healing DPNs can also recover other properties after damage that are equally critical to their overall performance. Yang et al. demonstrated an interesting example of this approach in their work to improve the output efficiency of solar cells in overcast weather by coating them with a transparent TENG that harvested energy from rain drops.^[45] The triboelectric layer was synthesised by cross-linking amine functional

PDMS with 1,4-phthalaldehyde, to form a dynamic imine network (SH-PDMS). A high transparency for the TENG was essential, so as not to limit the harvesting ability of the solar cell, and the transmittance of the virgin SH-PDMS was recorded to be >96% over the wavelength range of 400–800 nm. Furthermore, the self-healing properties provided by the DPN enabled full recovery of optical transmittance within two hours at room temperature after the introduction of damage. In simulations of the electric output of the device, water droplets falling from a height of 30 cm onto $8 \times 8 \text{ cm}^2$ sections of the TENG were found to generate a $V_{oc} = 6 \text{ V}$ and an $I_{sc} = 0.8 \mu\text{A}$, and this was only slightly reduced to $V_{oc} = 5.6 \text{ V}$ and $I_{sc} = 0.7 \mu\text{A}$ after self-healing.

Recently, Deng et al. extended the range of DPNs used in TENG devices by incorporating both β -hydroxy ester and disulfide groups that exchange through an associative mechanism, which are illustrated in Figure 1b.^[43] Here, silver nanowires were used as the electrode material, which were embedded in the disulfide epoxy-acid network. In this device, periodic contact with PTFE produced a V_{oc} of 26 V. These materials were able to fully restore their mechanical and energy harvesting properties within four hours after damage, and the interfacial healing also allowed the functional material to be built up from small pieces, so that a multitude of shapes and designs could be fabricated from the manufacture of identical TENG “bricks”, as demonstrated in Figure 4c. Guan et al. developed a similar TENG device, where disulfide bonds were incorporated into an amine-cured epoxy network.^[46] In this case the electrode layer was a dynamic epoxy network loaded with CNTs, and these networks could rapidly self-heal after damage, or be combined with additional TENG sections by irradiation with NIR, due to the high infra-red absorbance of CNTs. In addition to facilitating the construction of TENG devices from the combination of small elements, TENGs fabricated from associative DPNs also exhibit a high tensile strength.^[47] The higher energy typically required to induce exchange in these systems can also allow for greater selectivity over the self-healing conditions, allowing for a larger temperature window for stable operation.

5. Energy Storage

The electrical output from TENG devices can vary over time due to changes in ambient vibration or deformation levels. As a result, to ensure the electrical components of soft machines have a consistent power supply, the energy generated by a TENG must be stored.^[48] Compliant energy storage devices (ESDs), such as flexible supercapacitors or batteries, are ideally suited for this purpose, however, the complexity of these

devices poses specific challenges since all of their individual components (i.e., electrodes, electrolytes, separators, and current collectors) must be flexible, whilst retaining a high energy density device that remains safe during operation. State-of-the-art liquid electrolytes, while flexible, pose safety concerns when used in flexible devices, due to the flammable and volatile organic solvents that they contain.^[49] Safety can be improved by replacing them with solid-state electrolytes (SSEs), which reduces the risk of toxic leakage. However, these materials can suffer from low ionic conductivity, electrochemical instability, and poor mechanical properties.^[50]

A growing number of reports are demonstrating that the incorporation of DPNs into SSEs improves performance. For example, Huang et al. developed a PVA/zinc trifluoromethanesulfonate ($\text{Zn}(\text{CF}_3\text{SO}_3)_2$) hydrogel SSE for a self-healing zinc-ion battery (ZIB), which is shown in Figure 5a.^[51] This electrolyte had an extremely high ionic conductivity of up to 12.6 S cm^{-1} due to its porous 3D structure, and the supra-molecular interactions in the hydrogel network facilitated strong interfacial bonding to the zinc foil anode and polyaniline cathode, allowing for 1000 charge–discharge cycles with little change in coulombic efficiency (100%) or specific capacity (97.1%), as shown in Figure 5b. Moreover, the specific capacity of the zinc-ion battery was maintained even after three cutting and self-healing cycles. Similar results

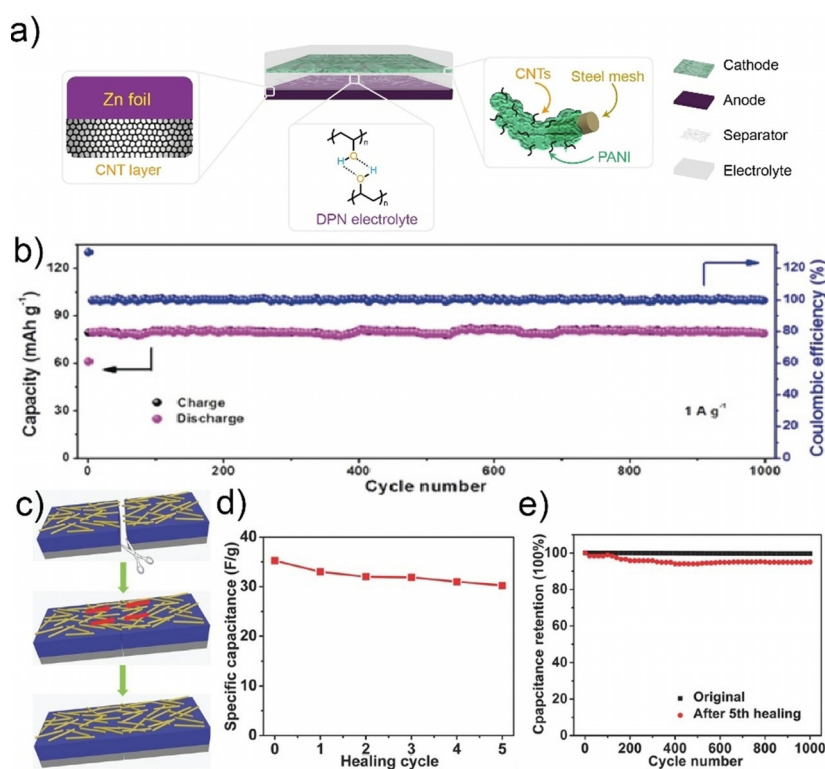


Figure 5. a) Diagram of integrated zinc-ion battery flexible ESD; b) cycling performance of zinc-ion battery containing a DPN solid state electrolyte, adapted with permission from Ref. [51]; c) illustration of a DPN electrode substrate for flexible ESDs restoring conductivity after damage; d) specific capacitance of a flexible supercapacitor after multiple self-healing cycles; e) capacitance retention of a supercapacitor after 1000 charge–discharge cycles, in addition to a supercapacitor that has been subjected to five self-healing cycles, adapted with permission from Ref. [59].

were achieved in a self-healing SSE for lithium-ion batteries (LIBs), through the incorporation of UPy-functionalised SiO₂ nanoparticles in a polyethylene glycol (PEG)–UPy matrix.^[52] Here, the quadruple hydrogen bonds between UPy groups in the system allowed for a homogeneous dispersion of the nanofiller, which improved the ionic conductivity, and provided excellent adhesion to the electrode materials. However, hydrogel SSEs often suffer from poor mechanical properties, even after the incorporation of dynamic covalent bonds, such as disulfides,^[53] imines, and boroxines.^[54] The ability to successfully balance good mechanical properties with high ionic conductivity is challenging in hydrogels,^[55] since increasing their cross-link density often retards the movement of ions.^[56] Potential solutions to this issue are emerging with development of double network hydrogels for SSEs, where a supramolecular network is interpenetrated within a covalent network,^[57] or through the incorporation of nanofillers with a unique architecture and porosity, allowing for the absorption of low-volatility ionic conductors, such as ionic liquids, as well as increasing the mechanical robustness of the SSE.^[58]

The layering of conductive materials on a DPN substrate can be an alternative approach to maintaining electrical properties and improving the safety of flexible ESDs.^[59] A supercapacitor fabricated by depositing CNTs onto a supramolecular network was able to restore its electrical properties after damage, and this was due to the lateral movement within the polymeric substrate reconnecting the separated areas of the CNT layer, as illustrated in Figure 5c.^[59] Figure 5d shows that the specific capacitance of the device was restored to 85.7% of its original value after being cut and self-healed five times, and there was little difference in the long-term stability of the device after self-healing, with only a 3.4% decrease in the specific capacitance of the device that had been self-healed five times after 1000 charge–discharge cycles, as shown in Figure 5e. The concept of DPN substrates in ESDs has also been demonstrated in LIBs, where the safety of the device was demonstrated by drilling a hole through it during operation.^[60] After drilling, the battery regained function in seconds, with no risk to safety.

6. Summary and Outlook

In this Minireview we have highlighted the synergistic effect of incorporating DPNs into components for soft machines. Until recently, research on DPNs has been primarily focussed on increasing the sustainability of materials, allowing for an extended service life through self-healing mechanisms, or creating materials with properties similar to thermosets while providing the reprocessing ability of thermoplastics. However, increasing work is emerging that demonstrates that the adaptive and responsive properties of DPNs can also provide an intriguing approach to gain access to a unique combination of multi-functional properties. These can include increased dielectric properties, enhanced conductivity, shape memory, or stimuli-responsive mechanical or electrical properties. The advances made in this new research area can increase the feasibility of developing future smart

soft machines, however, there are still some outstanding challenges that should be considered.

Of primary concern for DPNs are their inferior mechanical properties, such as tensile strength and creep resistance, when compared with conventional thermosets. This inhibits their use in soft-machine applications when large mechanical stresses or structural stability are required. Associative DPNs show the most promise in resolving these issues, due to their constant cross-link density, and recent work has shown that including different bonds capable of associative exchange in a single network can increase the tensile strength of DPN elastomers.^[61] However, in these systems care must be taken to ensure that cross-reactions do not occur between the different groups, which could result in the formation of a permanently cross-linked network. Creep resistance has also been increased in associative DPNs by including up to 40 mol% of permanent covalent bonds,^[8b] or by the incorporation of bonds with different exchange mechanisms, such as supramolecular interactions.^[62] Interestingly, the creep resistance of associative DPNs is also increased when the exchangeable groups are confined to a single block of a block copolymer, when compared with statistical polymers of identical monomer composition and molecular weight.^[63]

The synthesis of (multi-)block copolymers has been greatly simplified over recent years, in particular due to the significant advances in reversible-deactivation radical polymerisation (RDRP) techniques. The high degree of control RDRP provides over the molecular weight, dispersity, and composition of block copolymers facilitates their self-assembly into highly ordered structures that can improve materials' properties, such as their ionic conductivity,^[64] relative permittivity,^[65] and dielectric breakdown strength.^[66] State-of-the-art polymer synthesis techniques also provide facile access to branched polymer architectures, such as stars and combs, which are not well studied in the field of DPNs, but would provide greater control over the loci of functionality in the network, and would allow for higher degrees of internal diffusion due to the lower intrinsic viscosities of these types of polymer. Combining these well-defined polymer synthesis methodologies with the chemistry of DPNs is an exciting prospect for the future development of soft machines, opening up a new horizon to smart and functional devices.

Conflict of interest

The authors declare no conflict of interest.

- [1] G. M. Whitesides, *Angew. Chem. Int. Ed.* **2018**, *57*, 4258–4273; *Angew. Chem.* **2018**, *130*, 4336–4353.
- [2] D. Chen, Q. Pei, *Chem. Rev.* **2017**, *117*, 11239–11268.
- [3] L. Hines, K. Petersen, G. Z. Lum, M. Sitti, *Adv. Mater.* **2017**, *29*, 1603483.
- [4] H. Wu, Y. Huang, F. Xu, Y. Duan, Z. Yin, *Adv. Mater.* **2016**, *28*, 9881–9919.
- [5] J. Biggs, K. Danielmeier, J. Hitzbleck, J. Krause, T. Kridl, S. Nowak, E. Orselli, X. Quan, D. Schapeler, W. Sutherland, J. Wagner, *Angew. Chem. Int. Ed.* **2013**, *52*, 9409–9421; *Angew. Chem.* **2013**, *125*, 9581–9595.

- [6] C. Tugui, G. T. Stiubianu, M. S. Serbulea, M. Cazacu, *Polym. Chem.* **2020**, *11*, 3271–3284.
- [7] P. Caspari, S. J. Dünki, F. A. Nüesch, D. M. Opris, *J. Mater. Chem. C* **2018**, *6*, 2043–2053.
- [8] a) J. J. Cash, T. Kubo, D. J. Dobbins, B. S. Sumerlin, *Polym. Chem.* **2018**, *9*, 2011–2020; b) L. Li, X. Chen, K. Jin, J. M. Torkelson, *Macromolecules* **2018**, *51*, 5537–5546.
- [9] P. Shieh, W. Zhang, K. E. L. Husted, S. L. Kristufek, B. Xiong, D. J. Lundberg, J. Lem, D. Veysset, Y. Sun, K. A. Nelson, D. L. Plata, J. A. Johnson, *Nature* **2020**, *583*, 542–547.
- [10] D. Montarnal, M. Capelot, F. Tournilhac, L. Leibler, *Science* **2011**, *334*, 965.
- [11] J. M. Winne, L. Leibler, F. E. Du Prez, *Polym. Chem.* **2019**, *10*, 6091–6108.
- [12] N. De Alwis Watuthantrige, B. Ahammed, M. T. Dolan, Q. Fang, J. Wu, J. L. Sparks, M. B. Zanjani, D. Konkolewicz, Z. Ye, *Mater. Horiz.* **2020**, *7*, 1581–1587.
- [13] S. Nevejans, N. Ballard, M. Fernández, B. Reck, S. J. García, J. M. Asua, *Polymer* **2019**, *179*, 121670.
- [14] B. Zhang, Z. A. Digby, J. A. Flum, E. M. Foster, J. L. Sparks, D. Konkolewicz, *Polym. Chem.* **2015**, *6*, 7368–7372.
- [15] a) W. Denissen, J. M. Winne, F. E. Du Prez, *Chem. Sci.* **2016**, *7*, 30–38; b) M. Guerre, C. Taplan, J. M. Winne, F. E. Du Prez, *Chem. Sci.* **2020**, *11*, 4855–4870; c) N. J. Van Zee, R. Nicolaÿ, *Prog. Polym. Sci.* **2020**, *104*, 101233; d) S. Wang, M. W. Urban, *Nat. Rev. Mater.* **2020**, *5*, 562–583; e) P. Chakma, D. Konkolewicz, *Angew. Chem. Int. Ed.* **2019**, *58*, 9682–9695; *Angew. Chem.* **2019**, *131*, 9784–9797; f) G. M. Scheutz, J. J. Lessard, M. B. Sims, B. S. Sumerlin, *J. Am. Chem. Soc.* **2019**, *141*, 16181–16196; g) F. Van Lijsebetten, J. O. Holloway, J. M. Winne, F. E. Du Prez, *Chem. Soc. Rev.* **2020**, *49*, 8425–8438.
- [16] a) Y. Wu, Y. Wei, Y. Ji, *Polym. Chem.* **2020**, *11*, 5297–5320; b) A. M. Wemyss, C. Bowen, C. Plesse, C. Vancaeyzeele, G. T. M. Nguyen, F. Vidal, C. Wan, *Mater. Sci. Eng. R* **2020**, *141*, 100561; c) L. Saunders, P. X. Ma, *Macromol. Biosci.* **2019**, *19*, 1800313.
- [17] C. B. Gale, M. A. Brook, A. L. Skov, *RSC Adv.* **2020**, *10*, 18477–18486.
- [18] H. Luo, X. Zhou, C. Ellingford, Y. Zhang, S. Chen, K. Zhou, D. Zhang, C. R. Bowen, C. Wan, *Chem. Soc. Rev.* **2019**, *48*, 4424–4465.
- [19] N. Ning, S. Li, H. Sun, Y. Wang, S. Liu, Y. Yao, B. Yan, L. Zhang, M. Tian, *Compos. Sci. Technol.* **2017**, *142*, 311–320.
- [20] a) C. Ellingford, A. M. Wemyss, R. Zhang, I. Prokes, T. Pickford, C. Bowen, V. A. Coveney, C. Wan, *J. Mater. Chem. C* **2020**, *8*, 5426–5436; b) C. Ellingford, R. Zhang, A. M. Wemyss, C. Bowen, T. McNally, E. Figiel, C. Wan, *ACS Appl. Mater. Interfaces* **2018**, *10*, 38438–38448; c) C. Ellingford, R. Zhang, A. M. Wemyss, Y. Zhang, O. B. Brown, H. Zhou, P. Keogh, C. Bowen, C. Wan, *ACS Appl. Mater. Interfaces* **2020**, *12*, 7595–7604; d) H. Sun, X. Liu, H. Yan, Z. Feng, B. Yu, N. Ning, M. Tian, L. Zhang, *Polymer* **2019**, *165*, 1–10; e) S. J. Dünki, F. A. Nüesch, D. M. Opris, *J. Mater. Chem. C* **2016**, *4*, 10545–10553; f) C. Ellingford, A. Pengchaichaoen, A. M. Wemyss, C. Wan, *J. Composites Sci.* **2020**, *4*, 25.
- [21] H. Sun, X. Liu, S. Liu, B. Yu, N. Ning, M. Tian, L. Zhang, *Chem. Eng. J.* **2020**, *384*, 123242.
- [22] W. Hu, Z. Ren, J. Li, E. Askounis, Z. Xie, Q. Pei, *Adv. Funct. Mater.* **2015**, *25*, 4827–4836.
- [23] H. Sun, C. Jiang, N. Ning, L. Zhang, M. Tian, S. Yuan, *Polym. Chem.* **2016**, *7*, 4072–4080.
- [24] a) J. Van Damme, O. van den Berg, J. Brancart, L. Vlamincck, C. Huyck, G. Van Assche, B. Van Mele, F. Du Prez, *Macromolecules* **2017**, *50*, 1930–1938; b) A. M. Wemyss, K. Razmkhah, N. P. Chmel, A. Rodger, *Analyst* **2018**, *143*, 5805–5811.
- [25] S. Huang, Y. Liu, Y. Zhao, Z. Ren, C. F. Guo, *Adv. Funct. Mater.* **2019**, *29*, 1805924.
- [26] Z. Zhu, A. G. Einset, C.-Y. Yang, W.-X. Chen, G. E. Wnek, *Macromolecules* **1994**, *27*, 4076–4079.
- [27] M. Tang, P. Zheng, K. Wang, Y. Qin, Y. Jiang, Y. Cheng, Z. Li, L. Wu, *J. Mater. Chem. A* **2019**, *7*, 27278–27288.
- [28] T. Stukenbroeker, W. Wang, J. M. Winne, F. E. Du Prez, R. Nicolaÿ, L. Leibler, *Polym. Chem.* **2017**, *8*, 6590–6593.
- [29] H. Guo, Y. Han, W. Zhao, J. Yang, L. Zhang, *Nat. Commun.* **2020**, *11*, 2037.
- [30] R. Green, *Nat. Biomed. Eng.* **2019**, *3*, 9–10.
- [31] D. L. Taylor, M. i h. Panhuis, *Adv. Mater.* **2016**, *28*, 9060–9093.
- [32] Y. Guan, Y. Zhang, *Chem. Soc. Rev.* **2013**, *42*, 8106–8121.
- [33] A. P. Bapat, B. S. Sumerlin, A. Sutti, *Mater. Horiz.* **2020**, *7*, 694–714.
- [34] D. Wei, H. Wang, J. Zhu, L. Luo, H. Huang, L. Li, X. Yu, *Macromol. Mater. Eng.* **2020**, *305*, 2000018.
- [35] X. Xu, F. A. Jerca, V. V. Jerca, R. Hoogenboom, *Adv. Funct. Mater.* **2019**, *29*, 1904886.
- [36] a) K. Zhang, Y. Liu, Z. Wang, C. Song, C. Gao, Y. Wu, *Eur. Polym. J.* **2020**, *134*, 109857; b) J. Zhang, Z. Lei, S. Luo, Y. Jin, L. Qiu, W. Zhang, *ACS Appl. Nano Mater.* **2020**, *3*, 4845–4850; c) Z. Zou, C. Zhu, Y. Li, X. Lei, W. Zhang, J. Xiao, *Sci. Adv.* **2018**, *4*, eaq0508.
- [37] Z. Pei, Y. Yang, Q. Chen, E. M. Terentjev, Y. Wei, Y. Ji, *Nat. Mater.* **2014**, *13*, 36–41.
- [38] H. Wang, Y. Yang, M. Zhang, Q. Wang, K. Xia, Z. Yin, Y. Wei, Y. Ji, Y. Zhang, *ACS Appl. Mater. Interfaces* **2020**, *12*, 14315–14322.
- [39] F.-R. Fan, Z.-Q. Tian, Z. L. Wang, *Nano Energy* **2012**, *1*, 328–334.
- [40] a) V.-T. Bui, Q. Zhou, J.-N. Kim, J.-H. Oh, K.-W. Han, H.-S. Choi, S.-W. Kim, I.-K. Oh, *Adv. Funct. Mater.* **2019**, *29*, 1901638; b) V.-T. Bui, J.-H. Oh, J.-N. Kim, Q. Zhou, D. P. Huynh, I.-K. Oh, *Nano Energy* **2020**, *71*, 104561.
- [41] X. Dai, L. B. Huang, Y. Du, J. Han, Q. Zheng, J. Kong, J. Hao, *Adv. Funct. Mater.* **2020**, *30*, 1910723.
- [42] H. Chen, J. J. Koh, M. Liu, P. Li, X. Fan, S. Liu, J. C. C. Yeo, Y. Tan, B. C. K. Tee, C. He, *ACS Appl. Mater. Interfaces* **2020**, *12*, 31975–31983.
- [43] J. Deng, X. Kuang, R. Liu, W. Ding, A. C. Wang, Y. C. Lai, K. Dong, Z. Wen, Y. Wang, L. Wang, H. J. Qi, T. Zhang, Z. L. Wang, *Adv. Mater.* **2018**, *30*, 1705918.
- [44] J. Wang, J. Shi, X. Deng, L. Xie, J. Jiang, J. Tang, J. Liu, Z. Wen, X. Sun, K. Liu, Y. Fang, *Nano Energy* **2020**, *78*, 105348.
- [45] D. Yang, Y. Ni, H. Su, Y. Shi, Q. Liu, X. Chen, D. He, *Nano Energy* **2021**, *79*, 105394.
- [46] Q. Guan, Y. Dai, Y. Yang, X. Bi, Z. Wen, Y. Pan, *Nano Energy* **2018**, *51*, 333–339.
- [47] T. Patel, M. P. Kim, J. Park, T. H. Lee, P. Nallepalli, S. M. Noh, H. W. Jung, H. Ko, J. K. Oh, *ACS Nano* **2020**, *14*, 11442–11451.
- [48] Y. Zi, J. Wang, S. Wang, S. Li, Z. Wen, H. Guo, Z. L. Wang, *Nat. Commun.* **2016**, *7*, 10987.
- [49] E. Quartarone, P. Mustarelli, *J. Electrochem. Soc.* **2020**, *167*, 050508.
- [50] X. Wang, X. Lu, B. Liu, D. Chen, Y. Tong, G. Shen, *Adv. Mater.* **2014**, *26*, 4763–4782.
- [51] S. Huang, F. Wan, S. Bi, J. Zhu, Z. Niu, J. Chen, *Angew. Chem. Int. Ed.* **2019**, *58*, 4313–4317; *Angew. Chem.* **2019**, *131*, 4357–4361.
- [52] B. Zhou, Y. H. Jo, R. Wang, D. He, X. Zhou, X. Xie, Z. Xue, *J. Mater. Chem. A* **2019**, *7*, 10354–10362.
- [53] Y. H. Jo, S. Li, C. Zuo, Y. Zhang, H. Gan, S. Li, L. Yu, D. He, X. Xie, Z. Xue, *Macromolecules* **2020**, *53*, 1024–1032.
- [54] S. Li, C. Zuo, Y. H. Jo, S. Li, K. Jiang, L. Yu, Y. Zhang, J. Wang, L. Li, Z. Xue, *J. Membr. Sci.* **2020**, *608*, 118218.
- [55] P. Calvert, *Adv. Mater.* **2009**, *21*, 743–756.
- [56] a) B. Depalle, Z. Qin, S. J. Shefelbine, M. J. Buehler, *J. Mechanical Behavior Biomedical Mater.* **2015**, *52*, 1–13; b) W.-K. Shin, J.

- Cho, A. G. Kannan, Y.-S. Lee, D.-W. Kim, *Sci. Rep.* **2016**, *6*, 26332.
- [57] N. Sun, F. Lu, Y. Yu, L. Su, X. Gao, L. Zheng, *ACS Appl. Mater. Interfaces* **2020**, *12*, 11778–11788.
- [58] B. P. Thapaliya, C.-L. Do-Thanh, C. J. Jafta, R. Tao, H. Lyu, A. Y. Borisevich, S.-z. Yang, X.-G. Sun, S. Dai, *Batteries Supercaps* **2019**, *2*, 985–991.
- [59] H. Wang, B. Zhu, W. Jiang, Y. Yang, W. R. Leow, H. Wang, X. Chen, *Adv. Mater.* **2014**, *26*, 3638–3643.
- [60] Y. Zhao, Y. Zhang, H. Sun, X. Dong, J. Cao, L. Wang, Y. Xu, J. Ren, Y. Hwang, I. H. Son, X. Huang, Y. Wang, H. Peng, *Angew. Chem. Int. Ed.* **2016**, *55*, 14384–14388; *Angew. Chem.* **2016**, *128*, 14596–14600.
- [61] Y. Yang, L. Huang, R. Wu, W. Fan, Q. Dai, J. He, C. Bai, *ACS Appl. Mater. Interfaces* **2020**, *12*, 33305–33314.
- [62] S. Wang, S. Ma, Q. Li, X. Xu, B. Wang, K. Huang, Y. Liu, J. Zhu, *Macromolecules* **2020**, *53*, 2919–2931.
- [63] J. J. Lessard, G. M. Scheutz, S. H. Sung, K. A. Lantz, T. H. Epps, B. S. Sumerlin, *J. Am. Chem. Soc.* **2020**, *142*, 283–289.
- [64] K. Nakabayashi, A. Umeda, Y. Sato, H. Mori, *Polymer* **2016**, *96*, 81–93.
- [65] Z. Ma, Y. Xie, J. Mao, X. Yang, T. Li, Y. Luo, *Macromol. Rapid Commun.* **2017**, *38*, 1700268.
- [66] S. P. Samant, C. A. Grabowski, K. Kisslinger, K. G. Yager, G. Yuan, S. K. Satija, M. F. Durstock, D. Raghavan, A. Karim, *ACS Appl. Mater. Interfaces* **2016**, *8*, 7966–7976.

Manuscript received: September 30, 2020

Revised manuscript received: December 7, 2020

Accepted manuscript online: January 7, 2021

Version of record online: February 11, 2021